

Electronic Supporting Information

Ratiometric Fluorescent Nanosensors for Ultra-sensitive Detection of Mercury ion based on AuNCs/ MOFs

Xi-Jin Wu, Fan Kong, Chun-Qing Zhao and Shou-Nian Ding*

Jiangsu Province Hi-Tech Key Laboratory for Bio-medical Research, School of Chemistry and
Chemical Engineering, Southeast University, Nanjing 211189, China.

*Corresponding authors. (S.-N. Ding) Fax: (+86) 25-52090621. E-mail: snding@seu.edu.cn

Contents

Figure S1. TEM images of GSH-AuNCs and size distributions.....	S1
Figure S2. Uv–vis absorption spectrum of GSH-AuNCs.....	S1
Figure S3. Fluorescent excitation and emission spectrum of GSH-AuNCs	S2
Figure S4. SEM image of MIL-68(In)-NH ₂	S2
Figure S5. FTIR spectra of MIL-68(In)-NH ₂	S3
Figure S6. Fluorescent emission spectrum of MIL-68(In)-NH ₂	S3
Figure S7. Zeta (ζ) potential results of AuNCs, MIL-68(In)-NH ₂ and AuNCs/MIL-68(In)-NH ₂	S4
Figure S8. Fluorescent intensity of AuNCs/MIL-68(In)-NH ₂ at different quality ratios between MIL-68(In)-NH ₂ and Au NCs.....	S4
Figure S9. Effect of different time and different temperature on fluorescent intensity of AuNCs/MIL-68(In)-NH ₂ incubate with cysteine..	S5
Figure S10. Effect of different cysteine concentration on fluorescent intensity of AuNCs/MIL-68(In)-NH ₂ incubate with cysteine.....	S6
Figure S11. Fluorescent detection of AuNCs/MIL-68(In)-NH ₂ /Cys at different pH value.....	S6
Figure S12. The design of the μPAD.....	S7
Figure S13. The dry μPAD before treated and after treated with AuNCs/MIL-68(In)-NH ₂ /Cys.....	S7

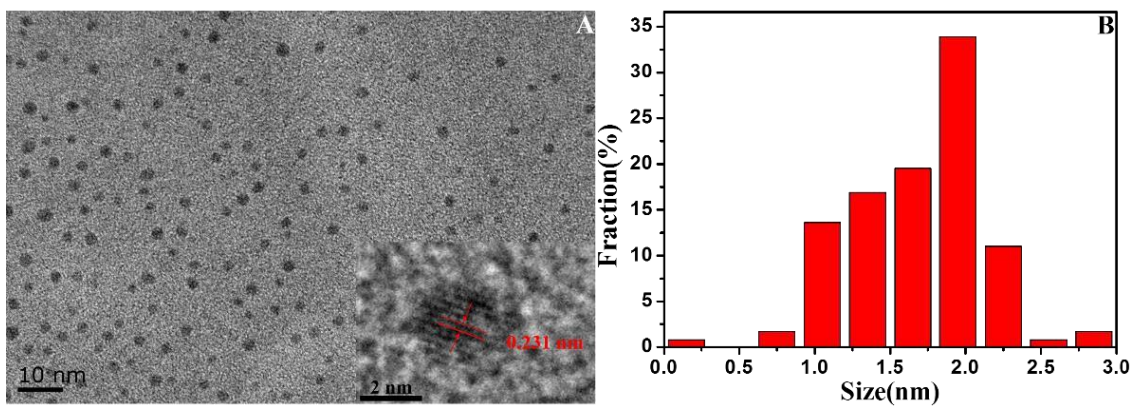


Figure S1. (A) TEM images of GSH-AuNCs (inset, HRTEM images of GSH-AuNCs, crystal lattice of a representative; scale bar, 2 nm) and (B) corresponding size distributions.

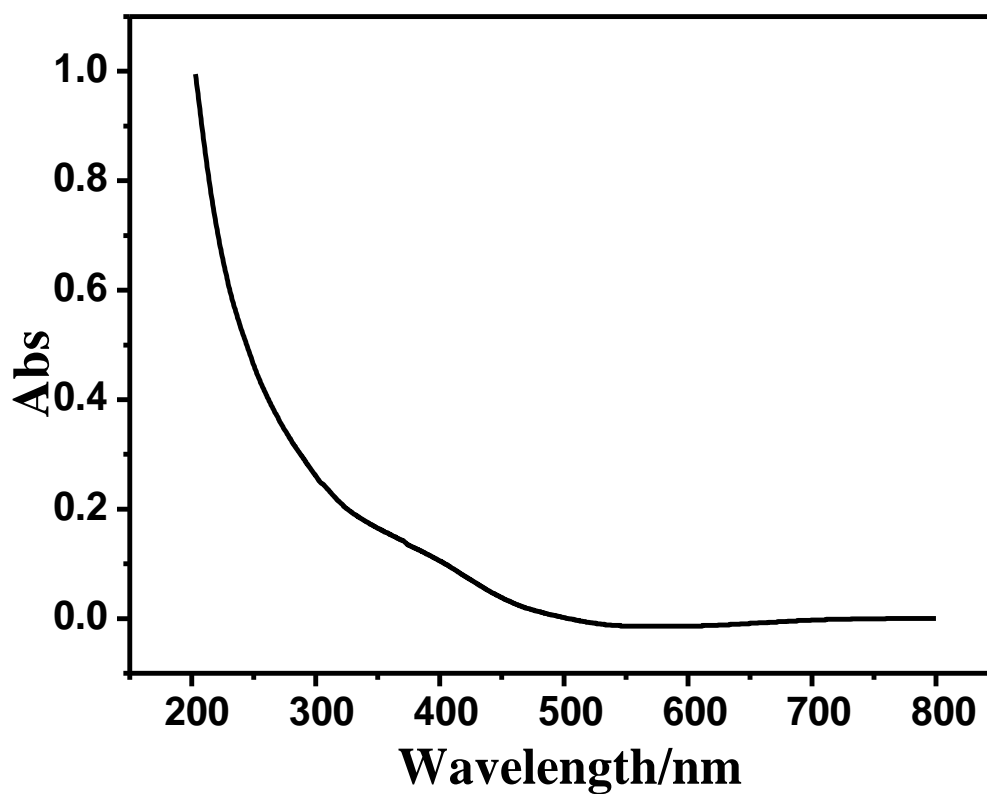


Figure S2. Uv-vis absorption spectrum of GSH-AuNCs.

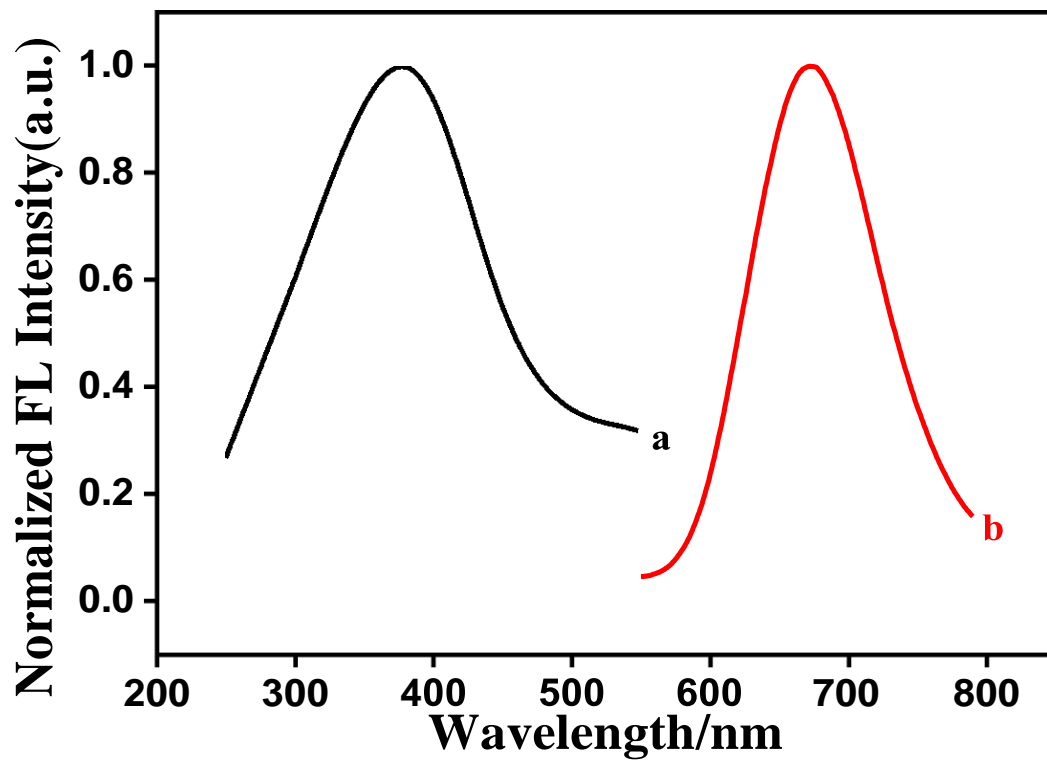


Figure S3. Fluorescent excitation (curve a), fluorescent emission (curve b) spectrum of GSH-AuNCs.

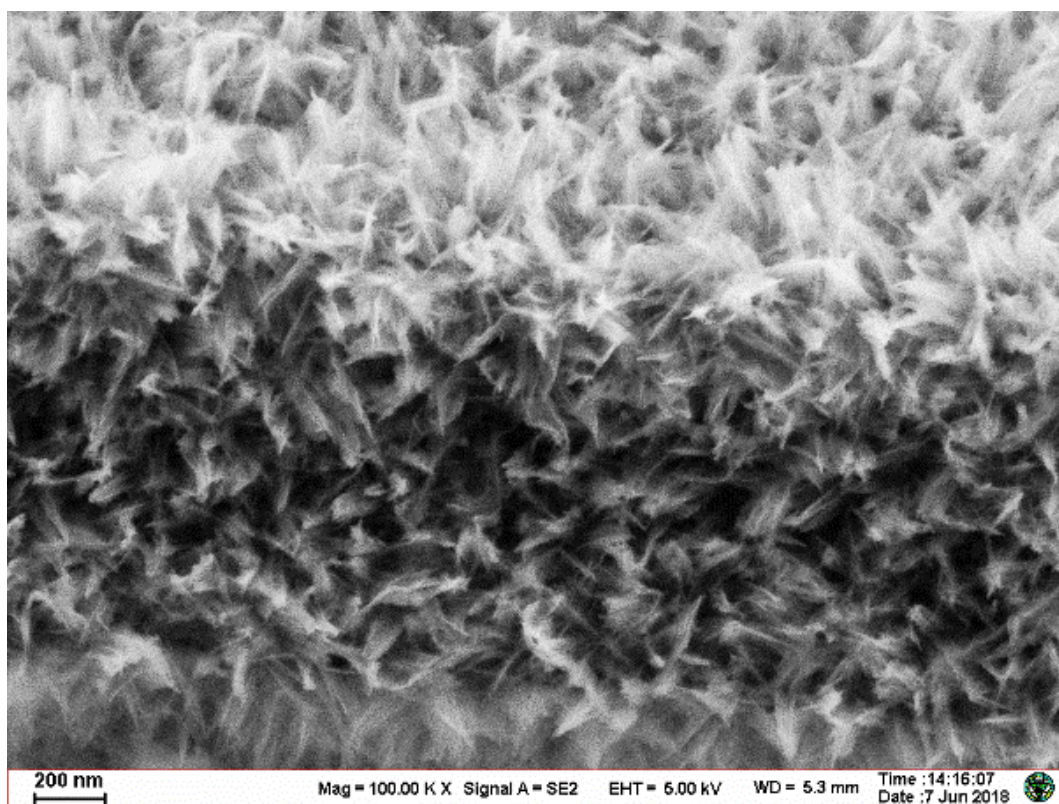


Figure S4. SEM image of MIL-68(In)-NH₂.

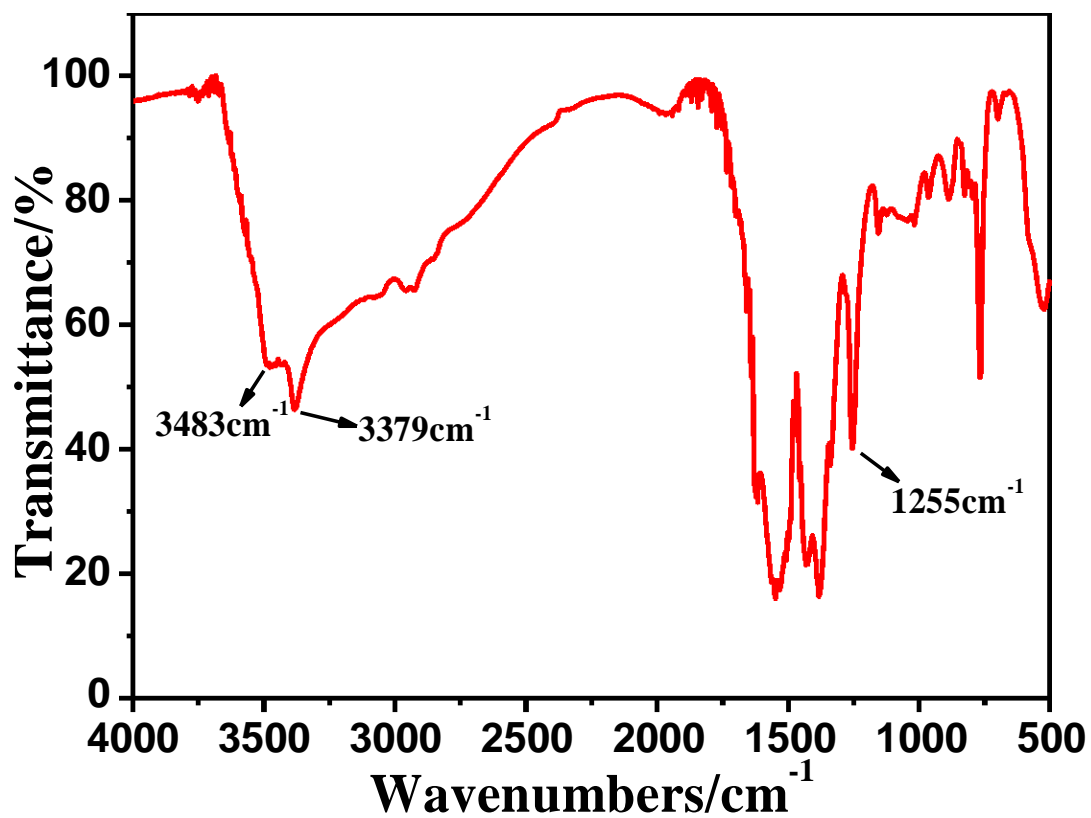


Figure S5. FTIR spectra of MIL-68(In)-NH₂

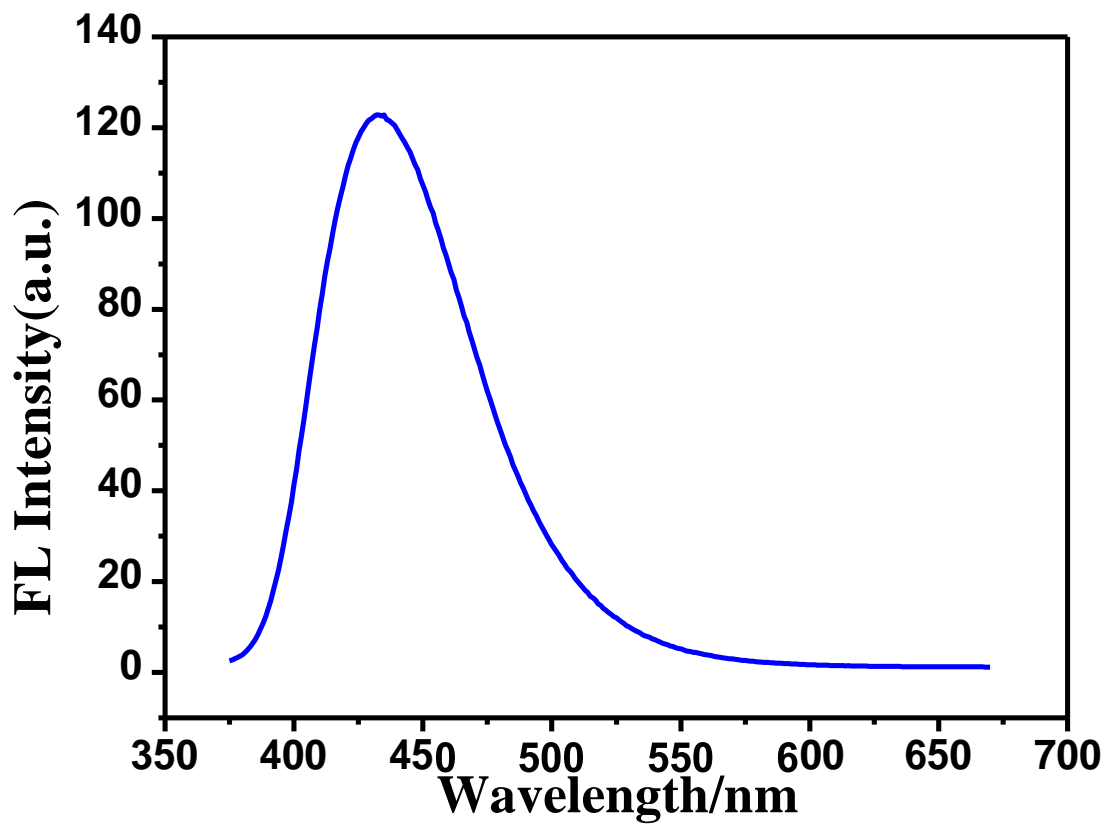


Figure S6. Fluorescent emission spectrum of MIL-68(In)-NH₂.

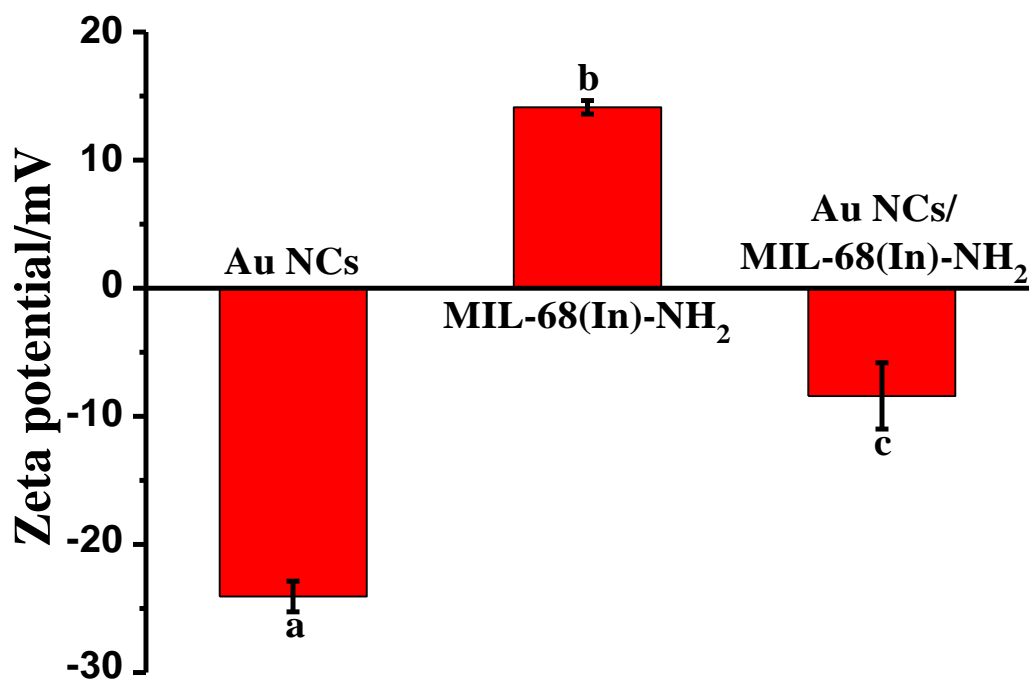


Figure S7. Zeta (ζ) potential results of AuNCs (a), MIL-68(In)-NH₂ (b) and AuNCs/MIL-68(In)-NH₂(c)

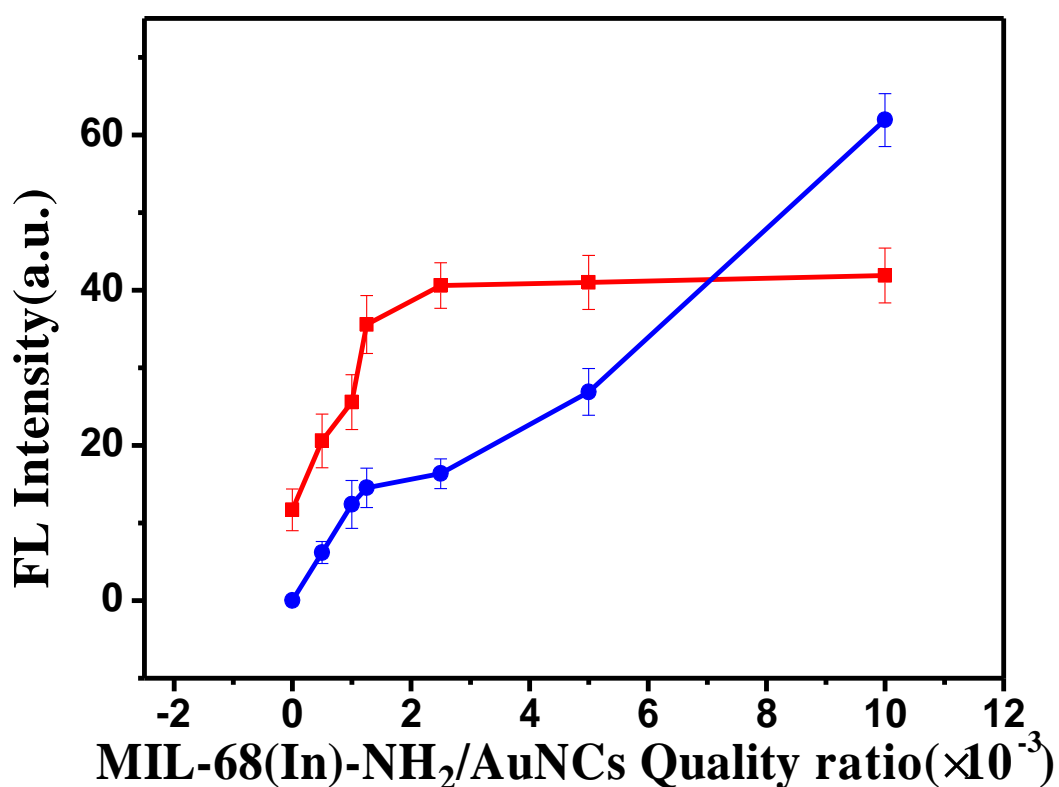


Figure S8. Fluorescent intensity of AuNCs/MIL-68(In)-NH₂ at different quality ratios between MIL-68(In)-NH₂ and Au NCs (A). The red curve represent the red fluorescent intensity of AuNCs/MIL-68(In)-NH₂ at 663 nm, and the blue curve represent the blue fluorescent intensity of AuNCs/MIL-68(In)-NH₂ at 438 nm.

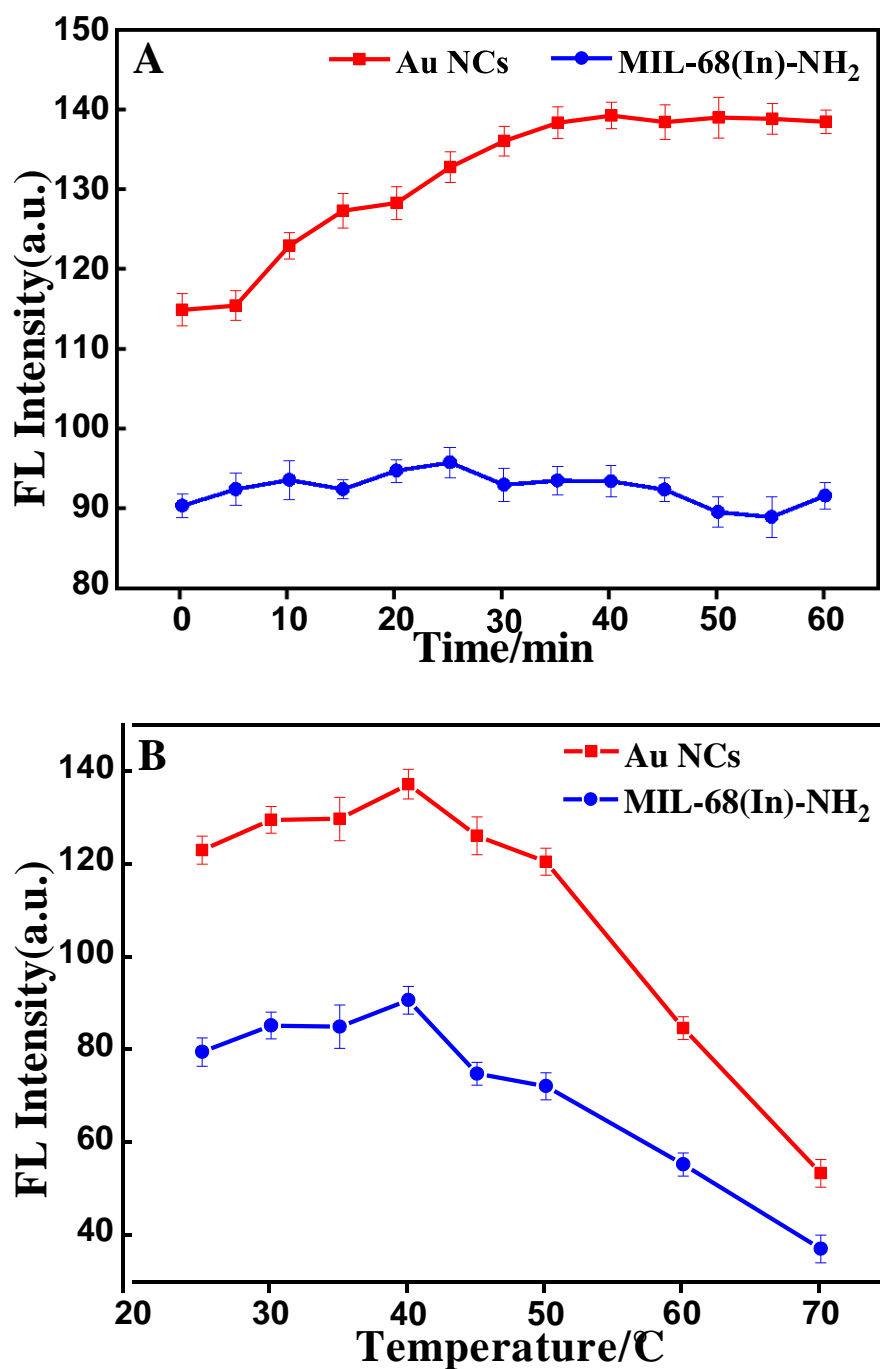


Figure S9. Effect of (A) different time and (B) different temperature on fluorescent intensity of AuNCs/MIL-68(In)-NH₂ incubate with cysteine. The red curves represent the red fluorescent intensity of AuNCs/MIL-68(In)-NH₂/Cys at 668 nm, and the blue curves represent the blue fluorescent intensity of AuNCs/MIL-68(In)-NH₂/Cys at 438 nm.

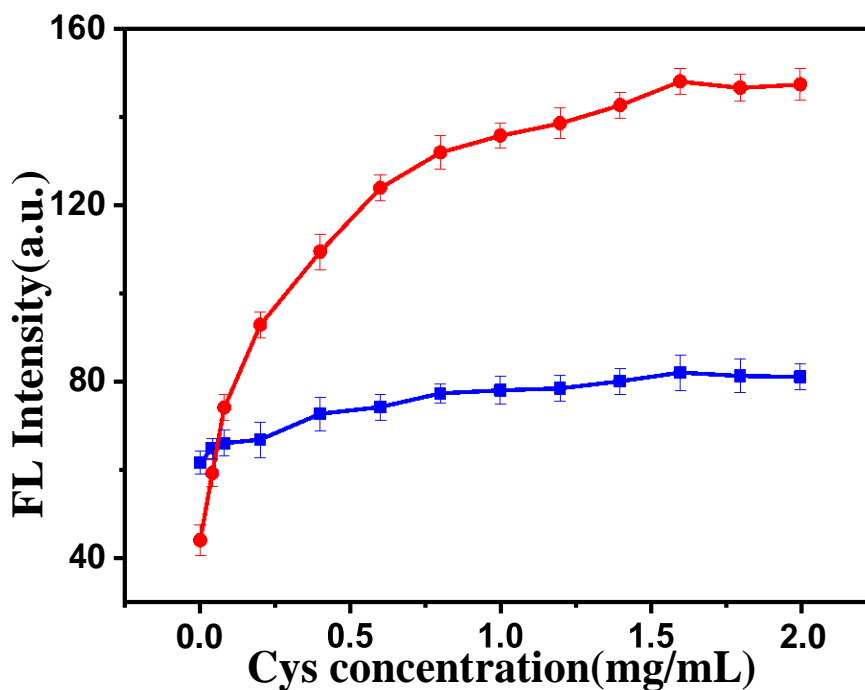


Figure S10. Effect of different cysteine concentration on fluorescent intensity of AuNCs/MIL-68(In)-NH₂ incubate with cysteine. The red curves represent the red fluorescent intensity of AuNCs/MIL-68(In)-NH₂/Cys at 668 nm, and the blue curves represent the blue fluorescent intensity of AuNCs/MIL-68(In)-NH₂/Cys at 438 nm.

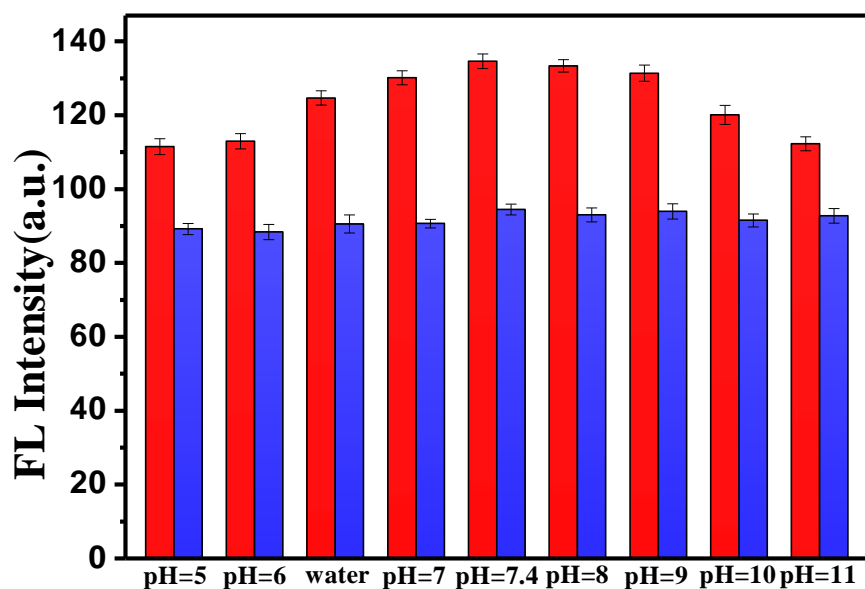


Figure S11. Fluorescent detection of AuNCs/MIL-68(In)-NH₂/Cys at different pH value. The red curves represent the red fluorescent intensity of AuNCs/MIL-68(In)-NH₂/Cys at 668 nm, and the blue curves represent the blue fluorescent intensity of AuNCs/MIL-68(In)-NH₂/Cys at 438 nm.

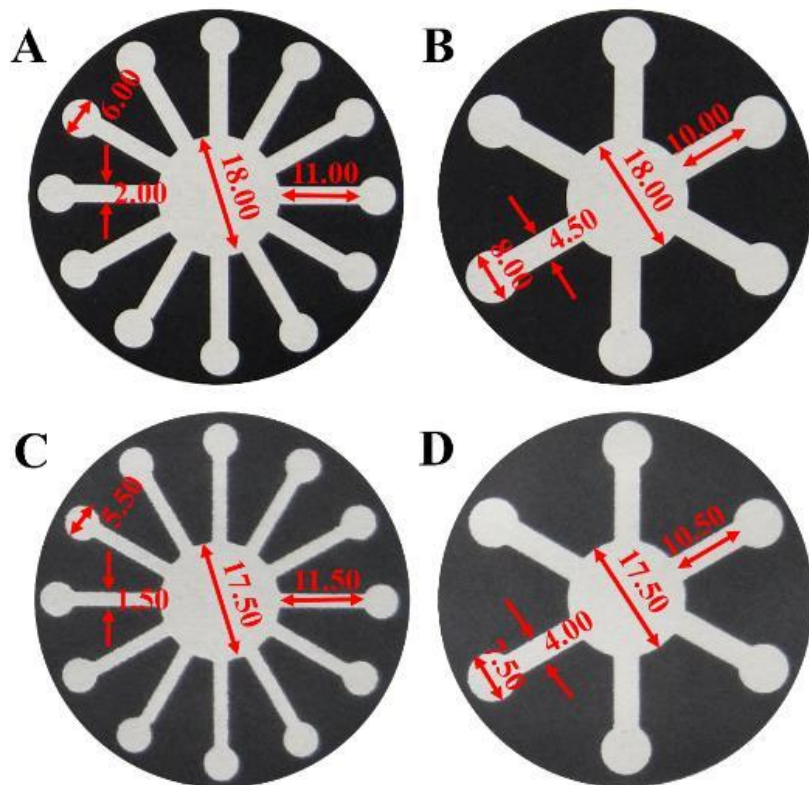


Figure S12. The design of the μ PAD. The lengths are showed in millimeters. The μ PAD (A) (B) before heating and (C) (D) after heating.

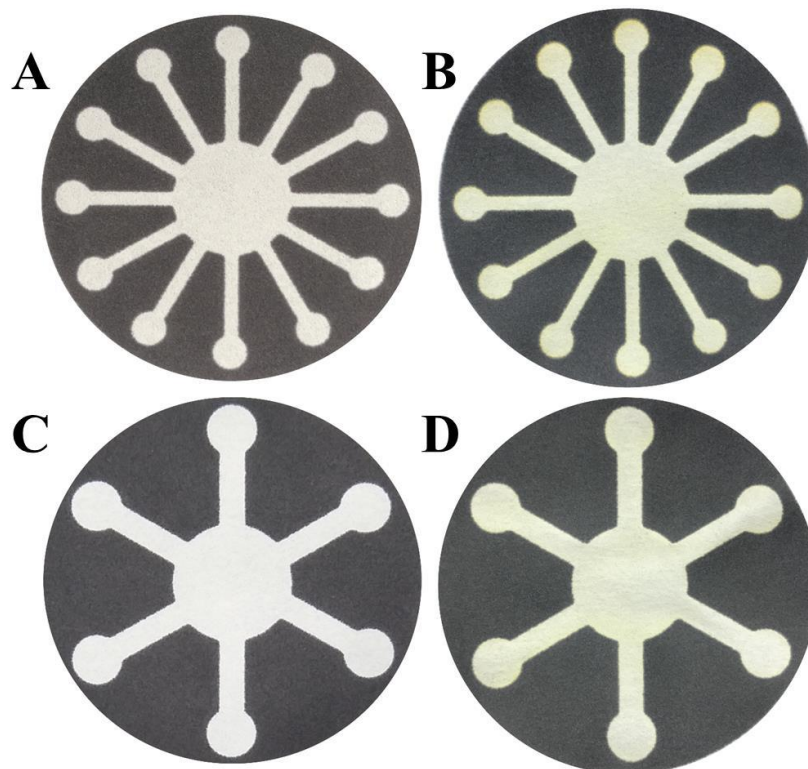


Figure S13. The dry μ PAD (A) (C) before treated with AuNCs/MIL-68(In)-NH₂/Cys and (B) (D) after treated with AuNCs/MIL-68(In)-NH₂/Cys.